Materials Advances

Accepted Manuscript

This article can be cited before page numbers have been issued, to do this please use: L. J. Briggs, M. Michie, J. Liu, D. Thomas, D. I. Cantor, J. Poole, T. Sutherland and C. L. Johnston, *Mater. Adv.*, 2026, DOI: 10.1039/D6MA00643D.

View Article Online
DOI: 10.1039/D6MA00643D

Recapitulating native aculeate silk structure enables enhanced mechanical performance in recombinant protein materials

Authors and Affiliations

Lyndall J. Briggs[1], Michelle Michie[1], Jian-Wei Liu[2], Denise Thomas[3], David Cantor[3], Jacinta Poole[4], Tara D. Sutherland[1], Caitlin L. Johnston[1]

[1] Health & Biosecurity, CSIRO, Canberra ACT, 2601, Australia

[2] Environment, CSIRO, Canberra ACT, 2601, Australia

[3] Australian Proteome Analysis Facility, Macquarie University NSW, 2109, Australia

[4] Manufacturing, CSIRO, Clayton VIC, 3169, Australia

View Article Online
DOI: 10.1039/D6MA00643D

Abstract

Recombinant structural proteins offer powerful and versatile platforms for the rational design of advanced functional materials, as their molecular architectures are genetically programmable and amenable to precise engineering. Among these systems, the coiled coil silk proteins of aculeate insects represent a distinctive class of polymers that combine efficient recombinant production with substantial sequence and structural design flexibility. While previous studies have demonstrated that materials fabricated from individual recombinant silk proteins can support diverse functional behaviours including nitric oxide sensing, oxygen reduction catalysis, photodynamic activity, and hydrogen evolution, their mechanical properties fall well short of those of native aculeate silk. Here, we show that recapitulating key features of the native silk architecture, specifically multi-protein assembly and covalent cross-linking, enables the formation of recombinant materials with enhanced mechanical performance relative to single protein recombinant silk materials. Materials incorporating all four silk proteins present in native aculeate silk (F1–F4) were rapidly stabilised using short, dry thermal treatments that induce intermolecular isopeptide cross-links while preserving the underlying coiled coil secondary structure. Compared with materials formed from single proteins and stabilised primarily by β-sheet interactions, these multi-component silk assemblies exhibit substantial but sample dependent increases in strength up to 200% and extensibility of up to 150%. Although the magnitude of improvement varies across samples, directly linking protein composition, cross-linking chemistry, and mechanical performance, this work demonstrates that cooperative multi-protein assembly and covalent network formation are critical determinants of native-like stability and resilience in aculeate silk. These findings establish recombinant multi-component aculeate silk materials as a robust and tunable platform for the development of mechanically resilient, multifunctional protein-based materials.

View Article Online
DOI: 10.1039/D6MA00643D

Introduction

Structural proteins represent a distinctive class of polymeric materials with exceptional potential for advanced materials design. Because their material properties are directly encoded by DNA sequence, structural proteins can be reproduced with high precision in recombinant systems, yielding polymers of uniform length and composition. Furthermore, modern molecular biology enables rational modification of these sequences, allowing new biological or chemical functionality to be engineered directly into the protein backbone. Together, these features position structural proteins as uniquely powerful templates for the development of programmable, multifunctional, and adaptive materials. Natural systems such as collagen and tropoelastin exemplify this paradigm, where multiple well-defined molecular interactions cooperate to generate robust material behaviour.[1-3]

Despite this promise, a persistent challenge in the field has been the inability to fully replicate the mechanical performance of native structural protein materials in recombinant formats.[4] This disconnect highlights a critical knowledge gap: while recombinant approaches excel at molecular-level precision and functionalisation, they often fail to capture the hierarchical architectures that underpin native mechanical properties.

In an effort to address this issue, our laboratory has examined a broad range of naturally occurring structural proteins[5] and identified the silk proteins from aculeate insects (bees, ants, and hornets) as particularly promising candidates.[6] Unlike silkworm and spider silks, which are dominated by β-sheet architectures,[7,8] native aculeate silks are composed of four distinct proteins (F1–F4)[9,10] that assemble into a heterotetrameric coiled coil structure.[11,12] These proteins are relatively short (300–350 amino acids), exhibit low sequence repetition, and are therefore well suited to recombinant production.[13] Honeybee silk proteins have been expressed at high yields in *Escherichia coli*,[14] readily purified via inclusion bodies, and refold efficiently into their native coiled coil structures following solubilisation.[15,16]

The amenability of aculeate silk proteins to recombinant production has enabled the development of a range of functional biomaterials to date. Most notably, efforts have focused on the F3 protein alone, which self-assembles into a coiled coil architecture that strongly binds heme cofactors. Exploiting this binding, F3-based materials have been engineered to incorporate heme and related porphyrins, enabling applications spanning nitric oxide biosensing for asthma diagnosis,[17-20] oxygen reduction catalysis as a platinum replacement in fuel cells,[21,22] photodynamic therapy,[23] and hydrogen evolution catalysis.[24] In these

View Article Online
DOI: 10.1039/D6MA00643D

single-protein materials, stabilisation is usually achieved by aqueous methanol treatment which promotes intermolecular β-sheet formation. Additional heat treatment can further introduce covalent cross-links into the resulting β-sheet-rich network. This approach differs fundamentally from native aculeate silk, which is stabilised mainly by covalent cross-linking while retaining a predominantly coiled coil architecture.

While these F3-based materials clearly demonstrate the functional versatility of recombinant aculeate silks, they represent only a partial reconstruction of the native system. Importantly, they do not replicate the mechanical properties of native aculeate silk.[25,26] Native honeybee silk, in contrast is composed of four proteins (F1-F4), and recombinant versions of these proteins have been demonstrated to assemble into a very stable antiparallel coiled coil configuration with a defined clockwise arrangement (F1-F3-F2-F4).[12] In the native silk these coiled coils are held together by covalent cross links.[13] This multi-component, covalently reinforced structure is likely central to the mechanical performance of the native material and yet has remained largely unexplored in recombinant material systems.

Here, we address this gap by fabricating silk materials that replicate the covalently linked heterotetrameric native aculeate silk architecture. We directly compare the physical and mechanical properties of these multi-protein, cross-linked materials with previously reported single-protein systems stabilised by β-sheet interactions. By reconstructing key aspects of the native hierarchy, this study provides new insight into how protein composition and cross-linking chemistry contribute to silk material performance and establishes design principles for engineering recombinant silk materials with native-like mechanical properties.

Experimental

Protein expression and purification

The F1 protein from *Apis mellifera* expresses poorly in transgenic *E. coli*. In contrast the *Apis dorsata* homolog expresses highly.[15] This homolog has 16 amino acid changes compared to the *Apis mellifera* F1, of which 9 are conserved in relation to volume and hydrophobicity, with all except one of these amino acid changes found in the AmelF1/AdorF1 homologs in other bee species, implying that there is sequence redundancy at these positions. Following an earlier study that found that the *Apis dorsata* F1 forms highly stable coiled coils with the *Apis mellifera* F2-4 silk proteins in solution[12] we generated materials from solutions of recombinant proteins containing the F1 from *Apis dorsata* and F2-4 from *Apis mellifera.*

View Article Online
DOI: 10.1039/D6MA00643D

Recombinant expression constructs for the four homologous honeybee silk genes (GenBank accession numbers: FJ235090 (AmelF2), FJ235091 (AmelF3), and codon optimised versions of AGZ15425.1 (AdorF1), KC708023 (AmelF4)) were transformed into *E. coli* BL21 (DE3) competent cells. Single colonies were inoculated into 10 mL Luria-Bertani (LB) medium containing the appropriate antibiotic and incubated at 37 °C with shaking for 4 hr. The starter culture was then transferred to 2 L shake flasks containing 500 mL Overnight Express™ Instant TB medium (Novagen) and grown at 37 °C for 18-20 hr with shaking at 200 rpm. Expressed proteins were harvested by centrifugation.[12,14,15] Inclusion bodies (IBs) were pretreated for 20 min at room temperature in lysis buffer supplemented with lysozyme (4 mL/g cell pellet; 100 mM Tris-HCl, pH 7.0; 5 mM EDTA; 5 mM DTT; 5 mM benzamidine HCl; 200 µg/mL lysozyme) and intermittent homogenisation using a stick blender. IBs were then isolated by centrifugation following additional mechanical cell lysis, which was performed by sonication (full power, 50% duty cycle, 5 sec pulses) and two passes through a high-pressure homogeniser (20,000 psi; Avestin Emulsiflex C3). IBs were washed three times with wash buffer (4 mL/g wet weight; 100 mM Tris-HCl, pH 7.0; 5 mM EDTA; 5 mM DTT; 2 M urea; 2% w/v Triton X-100), followed by a final wash without urea or Triton X-100. IBs were then rinsed in 1 M guanidine-HCl solution, solubilised in 8 M guanidine-HCl solution (3 mL/g IB), and insoluble material removed by centrifugation. The guanidinium concentration was reduced by dialysis using 10,000 MWCO Slide-A-Lyzer™ G3 cassettes (Thermo Scientific) against 100 volumes of water overnight at 4 °C. Silk proteins were purified by weak anion exchange on Fractogel® EMD DEAE resin (Merck) as previously described.[9] Proteins were then sterilised by passage through a 0.22 µm filter and protein concentration determined by BCA assay (Pierce).

Preparation of recombinant silk materials

Equimolar amounts of the four recombinant silk proteins were combined and concentrated to approximately 10 mg/mL using Vivaspin® 20 centrifugal concentrators with a 30,000 MWCO membrane (Sartorius). The protein solution was subsequently buffer exchanged into sterile water, with salt removal achieved through repeated dilution and concentration cycles in the centrifugal concentrator.

For films, 20-100 µL (0.2 - 1 mg protein) of the protein solution was cast onto a Teflon surface and allowed to dry overnight at ambient temperature producing transparent films (see

Results section). Post-drying, films were exposed to heat at approximately 115 °C or 190 °C for up to 4 days.

For fibres, the equimolar protein mixture was concentrated to 80 mg/mL to produce a viscous slightly yellow and transparent solution. Solutions were then extruded through an analytical syringe (Scientific Glass Engineering) using a syringe pump (KDScientific) at a rate of 12 mL/hr into coagulation solution comprising 53% methanol, 47% sodium phosphate buffer 50 mM pH 6.8 to form a continuous fibre. In this solution, the protein fibre started to coagulate after about 15 mm into the solution. After 1-2 hrs, the fibre was transferred to a storage solution of 80% methanol for at least 48 hr or until required. Fibre sections were then dried suspended over two points, then as required drawn to approximately x2 length until no further necking was observed in 80% methanol and heat-treated as described in Poole *et al*.[25]

Fourier-Transform Infrared Spectroscopy (FTIR)

Infrared spectra were acquired from films using a PerkinElmer Spectrum 2 FTIR spectrometer equipped with a diamond attenuated total reflectance (ATR) accessory. Spectra were recorded at room temperature over the range of 4000–400 cm^{-1} with a resolution of 2 cm^{-1} and five accumulations per sample. To compare samples, we calculated the ratio of coiled coil (signal at wavelength 1632-1652) to β-sheet (signal at wavelength 1610-1624) in the Amide I region, as previously characterised in Sutherland *et al*.[27]

Solubility and protease susceptibility assays

To assess solubility, treated films were submerged in 50 mM sodium phosphate buffer (pH 7.2) for 24 hr at room temperature. After incubation, the buffer was removed, and any remaining insoluble material was re-dried on a Teflon surface.

Protease susceptibility was evaluated by incubating treated films with 1 mg/mL trypsin (MP Biomedicals) at 37 °C. The silk proteins contain ample trypsin sites (F1:38; F2:29; F3:36; F4:35) and the entirety of each protein is digested to small peptides even in the material form.[9] Resistance to degradation was assessed as visible films or fragments that remained in the material form after trypsin exposure.

Identification of amino acid cross-links

Two methods were used to elucidate amino acid cross-links that arise due to heat treatment: amino acid analysis of heat-treated films compared to untreated control films and liquid

View Article Online
DOI: 10.1039/D6MA00643D

chromatography mass spectroscopy (LCMSMS) of heat-treated samples to identify cross-linked peptides.

Quantitative amino acid analysis by acid hydrolysis was conducted on heat-treated films (~190 °C for 10 min) and untreated controls at the Australian Proteome Analysis Facility, using duplicate measurements on three independent films. The concentrations of amino acids were determined using pre-column derivatisation amino acid analysis with 6-aminoquinolyl-N-hydroxysuccinimidyl carbamate (AQC)[28] followed by separation of the derivatives and quantification by modified reversed phase ultra performance liquid chromatography. Bovine serum albumin (BSA; Sigma) is used as a positive control for the effectiveness of reactions involving a hydrolysis step during the quantitative amino acid analysis. This procedure enables analysis of 16 of the 20 common proteinogenic amino acids. Sample was hydrolysed in HCl for 24 hr at 110 °C. An internal standard (Norvaline and α-amino butyric acid; Nva/AABA) was added to each sample following hydrolysis. Following a dilution in ultra-pure water, 10 µL of the solution was derivatised using an AccQ-Tag Ultra Derivatization Kit (Waters Corporation, Milford, Mass. USA) following suppliers recommended procedures. The use of HCl as the hydrolysis reagent converts asparagine and glutamine to their acid forms, aspartic acid and glutamic acid respectively. In the presence of HCl, the amino acid tryptophan is destroyed while cysteine/cystine are partially destroyed. Therefore, quantitation for these amino acids cannot be undertaken by this hydrolysis method. Deficits of amino acids in the treated samples relative to untreated samples were taken to indicate residues that had been modified by heat-treatment.

For LCMSMS analysis two sets of experiments were conducted. In one set, films were heat-treated at ~115 °C for 60 min, then solubilised in 50 mM sodium phosphate buffer (pH 7.2), and proteins separated by SDS-PAGE. Bands corresponding to oligomeric proteins were excised for LCMSMS. The second set included untreated films and films heat-treated at ~190 °C for 2 min.

Samples were digested with sequencing grade trypsin (Promega) then separated on a nano column (PepMap100 C18, 150 mm x 75 µm, 2 µm, ThermoScientific) using an UltimateTM 3000 RSLC nano LC system (ThermoScientific), ionized with a Nanospray Flex Ion Source (ThermoScientific) and tandem MS/MS analysis was performed using an Orbitrap Fusion MS (ThermoScientific) following the protocol described by Johnston *et al.*,[12] targeting masses equivalent to two tryptic peptides minus 18.0106 Da, indicative of water loss during amide bond formation, as previously reported for heat-treated silk films by Huson *et al.*[26] Candidate

View Article Online
DOI: 10.1039/D0MA00643D

cross-links were not identified on the basis of precursor mass alone; assignments were further supported by MS/MS fragmentation data, in which sequence-specific fragment ions confirmed peptide identity and the sites of cross-linking.

Mechanical testing of fibres

Fibres were mounted on paper frames with a 10 mm gap, fixed at either end using epoxy glue, with their diameter determined using an optical microscope (Leica Wild M3Z Kombistereo). Tensile measurements were carried out at a strain rate of 2.5 mm.min^{-1} on an Instron 5500R (Instron, USA) fitted with a 100 N static load cell. Tests were conducted in air at 23 °C and 50% relative humidity. Mechanical testing was performed on 33 fibre samples.

Results and Discussion

Modification of cross-linking in materials generated from all four silk proteins

Aculeate larvae can control the morphology of their silk during spinning to produce either fibers or films.[29] This silk comprises four proteins,[9] and silk from ants and bees is stabilised by interprotein isopeptide cross-links.[13] Previous studies have shown that the silk proteins express at high yields in standard *E. coli* expression systems[14,15] and can be readily purified from host cell proteins.[12] Protein films are straightforward to fabricate and therefore provide a convenient platform for systematically optimising isopeptide cross-linking in materials with the native protein composition. Accordingly, protein films approximately 6 mm in diameter (~1 mg protein per film) were generated from recombinantly produced and purified versions of all four naturally occurring honeybee silk proteins using a simple casting approach (Figure 1A). Similar cross-linking chemistry as that found in native silk has been observed following dry thermal treatment of recombinant F3 silk materials at 190 °C for 1 hr.[26] In the present study, films composed of F1-F4 silk proteins were subjected to thermal treatment at ~115 °C or ~190 °C (Figure 1A).

The extent of cross-linking was assessed using aqueous dissolvability and susceptibility to proteolytic degradation. In contrast to F3-only materials, which require 1 hr of treatment to become aqueous-insoluble,[26] materials composed of all four silk proteins became insoluble after only 1 min of thermal exposure at ~190 °C (Figure 1C), demonstrating that incorporation of all four silk proteins markedly accelerates thermally induced network formation consistent with formation of a more stable and tightly bound structure.[12]

View Article Online
DOI: 10.1039/D6MA00643D

Thermal treatment can, in principle, promote both protein aggregation/coagulation and covalent cross-link formation. FTIR analysis confirmed that these heat treatments had minimal impact on protein secondary structure. Across all conditions tested, spectra consistently exhibited a broad absorbance band between 1632-1652 cm^{-1}, characteristic of a coiled coil architecture (Figure 1B). This is inconsistent with extensive aggregation or protein denaturation, which would be expected to produce measurable structural rearrangements such as increased β-sheet content.

After thermal treatment at ~115 °C for equivalent times, all films remained soluble. However, SDS-PAGE analysis of the resolubilised proteins revealed, in addition to monomeric species migrating at the expected molecular weights (30–38 kDa), the presence of higher molecular mass bands consistent with the formation of covalently cross-linked oligomeric proteins. The formation of oligomeric species that persist under denaturing conditions during SDS–PAGE is consistent with covalent bonding rather than non-covalent aggregation. The relative abundance of these cross-linked species increased with longer thermal treatment durations (Figure 1D), demonstrating that although heating at ~115 °C for up to 1 hr was insufficient to generate an insoluble network, it is sufficient to initiate covalent intermolecular cross-linking. Films were then exposed for longer time periods at ~115 °C to determine how much cross-linking was required to generate insoluble material (Figure 1E). The amount of oligomeric species present in solubilised film samples increased up to 8 hr treatment, then decreased after 16 hr treatment coincident with the presence of insoluble material. By 48 hr most of the protein was cross-linked into an insoluble material. The formation of insoluble material with comparatively low levels of cross-linking is consistent with that found in native materials that have approximately one covalent cross-link between every tetramer.[13]

View Article Online
DOI: 10.1039/D6MA00643D

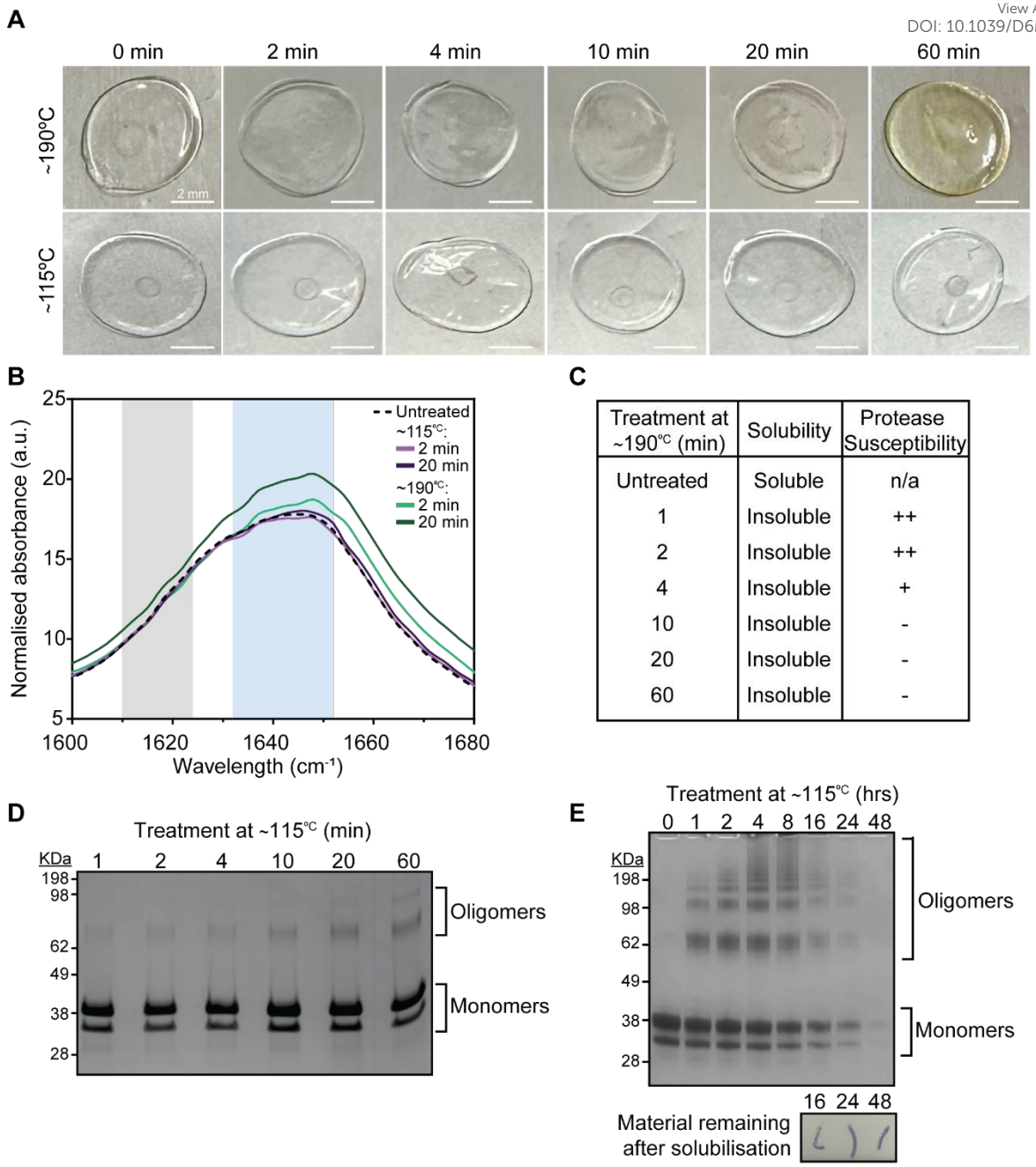

Figure 1. (A) Representative images of silk films composed of proteins F1-F4 after heat treatment at ~190 °C or 115 °C for up to 60 min. **(B)** Representative FTIR spectra from thermally treated films. Blue shaded: coiled coil (1632–1652 cm^{-1}); grey shaded: β-sheet (1610–1624 cm^{-1}) **(C)** Solubility and protease results from silk films generated from F1-F4 (+ indicates susceptibility to trypsin, - indicates resistance to trypsin). SDS-PAGE analysis showing monomeric proteins and the formation of oligomeric protein complexes in resolubilised F1-F4 silk materials after thermal treatment at ~ 115 °C for up to 60 min (**D**) or 48 hours (**E**) and insoluble material remaining after thermal treatment at ~115 °C.

View Article Online
DOI: 10.1039/D6MA00643D

Proteolytic degradation with trypsin was also used to assess the extent of cross-link network formation, as increased covalent cross-linking is expected to restrict enzyme access to cleavage sites. The silk proteins contain ample trypsin sites (F1:38; F2:29; F3:36; F4:35) and the entirety of each protein is expected to be digested to small peptides if these sites are available. Films treated at ~190 °C for 1 or 2 min remained susceptible to proteolytic degradation by trypsin (1 mg/mL, 37 °C, 1 hr). With increasing treatment time, resistance to digestion progressively increased: films treated for 4 min at ~ 190 °C exhibited only partial degradation, consistent with the onset of cross-linked network formation, whereas films treated for ≥ 10 min at ~190 °C showed no detectable proteolysis under the conditions tested (Figure 1C), indicative of a densely cross-linked, enzyme-resistant material. A similar trend was observed for insoluble films heated at ~ 115 °C (Figure 1E), albeit on a longer timescale. Films treated for 16 hr at ~115 °C were still degraded by trypsin (1 mg/mL, 37 °C, 1 hr), while 24 hr-treated films (~115 °C) required extended digestion (2 hr) for degradation. In contrast, films treated for longer durations were resistant to tryptic digestion, consistent with the gradual formation of a stable cross-linked network at lower temperature.

To support the formation of covalent isopeptide cross-links, two complementary analyses were performed: quantitative amino acid analysis following acid hydrolysis and LCMSMS analysis. Because acid hydrolysis cleaves peptide and isopeptide bonds but does not quantitatively regenerate amino acids that have participated in covalent cross-linking due to competing side reactions and degradation, thermally induced cross-links can be inferred indirectly from selective reductions in amino acid recovery. Amino acid analysis after acid digestion revealed that heat-treated films exhibited significant decreases in Glx (Gln + Glu), Lys, Ser, Asx (Asn + Asp), Thr and Phe relative to untreated controls (Figure 2). No significant differences were observed for Ala, Leu, Val, Arg, Ile, Gly or Pro. While the reduction in Phe was statistically significant, the absolute amounts were close to the limit of detection and are therefore unlikely to be biologically relevant (inset, Figure 2). The observed decreases in Glx, Lys, Ser, Asx and Thr are consistent with previous studies of thermally treated recombinant F3 silk, in which covalent cross-links were shown to form between Lys/Asn and Asp/Glu, or between Lys and Ser/Thr residues.[26] The selective depletion of residues known to participate in isopeptide bond formation, supports that the dominant and defining stabilisation mechanism is the formation of covalent isopeptide cross-links, rather than protein coagulation or aggregation.

View Article Online
DOI: 10.1039/D6MA00643D

To determine whether cross-linking was localised to specific residues or distributed throughout the protein structure, tryptic digestion followed by LCMSMS analysis was performed. Analyses were conducted on untreated films, films heat-treated at ~190 °C for 2 min (which were aqueous insoluble yet trypsin-susceptible; Figure 1), and cross-linked oligomeric species isolated following thermal treatment at ~115 °C (Figure 1D). Isopeptide cross-links were identified in all samples: two in untreated controls, 27 in the oligomeric protein species generated at ~115 °C, and 41 in films treated at ~190 °C (Supplementary Table 1). Cross-links were distributed across the protein sequence, with multiple instances of the same lysine residue forming covalent bonds with different glutamic acid, aspartic acid, serine or threonine residues, indicating largely non-specific cross-link formation.

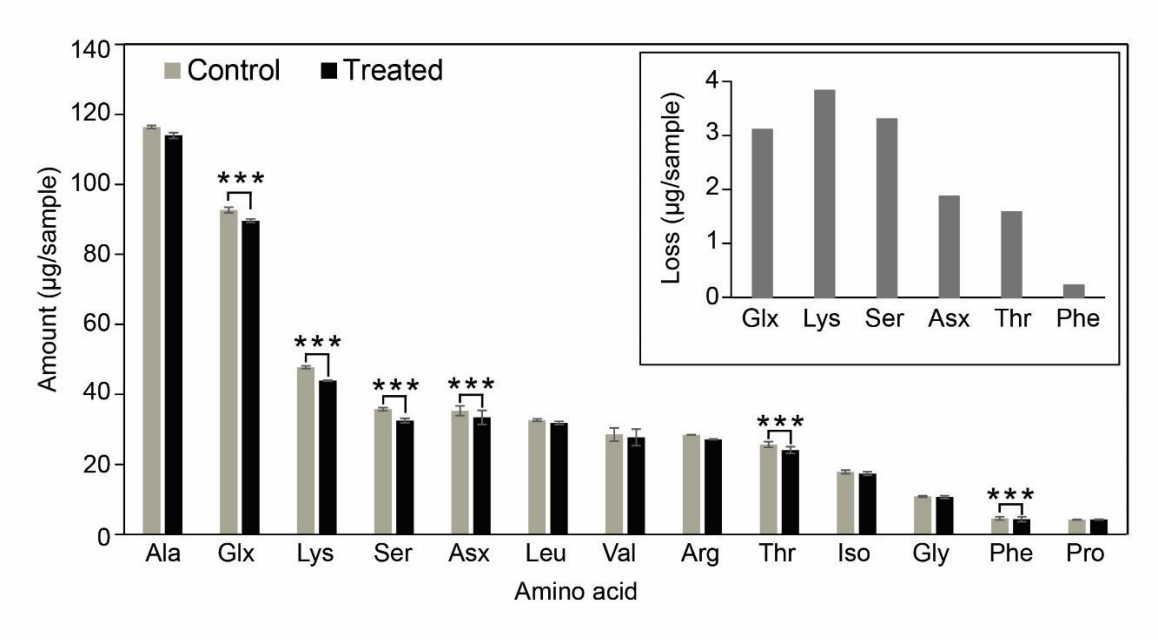

Figure 2. Results of quantitative amino acid analysis via acid hydrolysis. Error bars are standard deviation; significance determined by T-test (two tailed) and significance of p>0.05%. Inset shows the loss of amino acid per sample for those that had a significant change *** between treated (~190 °C for 10 min) and controls (no heat treatment).

View Article Online
DOI: 10.1039/D6MA00643D

Mechanical properties of materials generated from all four silk proteins

While protein films provide a convenient platform for controlling composition and optimising cross-linking chemistry, mechanical characterisation was performed using fibres. Fibre geometries are the standard format for tensile testing of protein and polymeric materials, enabling well-defined loading conditions and direct comparison with both native silks and prior recombinant systems. Fibres from solutions of recombinantly produced and purified F1-F4 proteins were generated and heat treated.

In line with previous methods, fibres were produced by extruding protein solutions through a fine-gauge needle into aqueous methanol, then suspending them between two points where they contracted and dried into finer filaments before being drawn.[14]

During drawing, the fibres exhibited clear necking behaviour, with necking initiating at multiple positions along the fibre length (Figure 3). The occurrence of multiple necking events during tensile deformation is unusual in engineering materials. Typically, necking initiates at a single location once the material reaches its ultimate tensile strength, after which deformation localises at that site until fracture. In contrast, multiple necking is more commonly observed in highly heterogeneous or textured polycrystalline materials under specific loading conditions, where microstructural heterogeneity or local imperfections can promote the formation of several necking regions.[30]

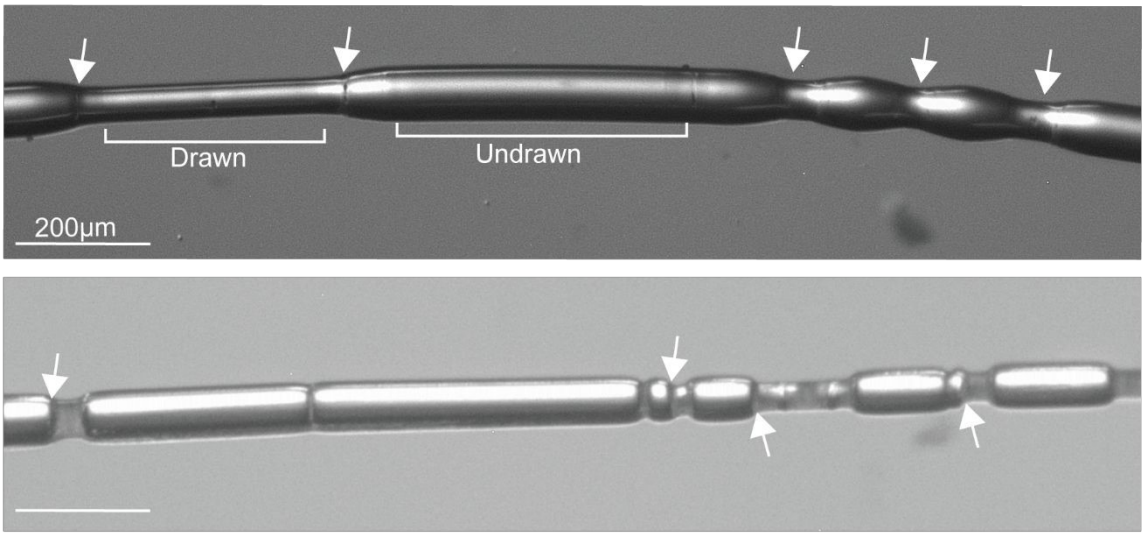

View Article Online
DOI: 10.1039/D6MA00643D

Figure 3. Light microscopy images of fibres fabricated from recombinant honeybee silk proteins showing fibres mid-draw with necking behaviour initiated at multiple points (*white arrows*). Scale bar: 200 µm.

The remarkable necking behaviour observed in these fibres can be explained by the exceptional stability of the F1-F4 coiled coil complex described recently by Johnston *et al.*.[12] In the F1-F4 materials, the stable, high-aspect-ratio coiled coils are fully retained during aqueous methanol treatment.[31] During fibre drying, predominantly transverse dehydration occurs as fibres are suspended between two points, which would promote organisation of these coiled coils into partially oriented smectic phases. Upon drawing, these smectic phases can readily align into a more crystalline material, with spatial variations in crystallinity within surrounding amorphous regions acting as stress concentrators during tensile deformation.

Necking initiated at multiple points was not observed in earlier studies with fibres generated from F3 alone. In these materials, methanol exposure during fibre processing induced a structural rearrangement from coiled coil to beta-sheet structure.[25-27] This methanol-induced structural rearrangement would be expected to reduce both the abundance and effective aspect ratio of coiled coil domains, which is expected to limit the formation of partially oriented smectic phases. In the F1-F4 fibres, retention of the coiled coil structure during aqueous methanol treatment is predicted to enhance anisotropic ordering upon drawing, providing a mechanistic explanation for the unusual multi-necking behaviour observed in these fibres.

The F1-F4 fibres, after drawing and cross-linking using heat treatment (~190 °C, 60 min), exhibited substantial variability in mechanical properties (Figure 4). There are many factors that could contribute to this variability including introduction of flaws during material handling (drawing, heating and mounting of samples) as well as the rate and extent of draw of the fibres. In this study, fibre drawing was performed manually and terminated once no further necking was observed, without systematic optimisation of the draw ratio. Consequently, the applied draw conditions were not uniform across samples. This lack of optimisation suggests that further improvements in mechanical performance would be achievable through controlled and optimised drawing protocols.

View Article Online
DOI: 10.1039/D6MA00643D

Many of the fibres fabricated in this study had higher tensile strength and elasticity than previously reported fibres produced from recombinant silk proteins (Figure 4). The tensile strength of many also exceeded that reported for native fibres, and although they were less brittle than those described by Zhang *et al.*,[32] they did not reach the extensibility reported by Hepburn *et al*.[33] As commonly observed in fibrous materials, a clear trade-off between strength and extensibility was evident, with stronger fibres exhibiting reduced strain to failure (Figure 4).

Indeed, based on optimised fibre production and drawing protocols[25] and the upper performance of the fibre samples (Figure 4) it is reasonable to predict that fibres with tensile strengths exceeding 350 MPa could be produced from this material. Notably, the strongest fibre measured in the present study reached 361 MPa, representing an approximately 200% increase relative to the maximum strength reported for fibres composed of F3 protein alone.[25]

In addition, the fibres produced in this study had diameters of 42 ± 2 μm. A very weak correlation between diameter and stress is apparent in our data set ($R^2 = 0.02$; Supplementary data Figure 1). Classical fracture mechanics and statistical size-effect models predict an inverse relationship between fibre diameter and tensile strength, a trend well established in glass, natural and polymer fibres. This behavior is also supported by silk-specific analyses demonstrating increased tensile strength with decreasing fibre diameter.[34] Accordingly, further reductions in fibre diameter are expected to yield additional enhancements in tensile performance.

.

View Article Online
DOI: 10.1039/D6MA00643D

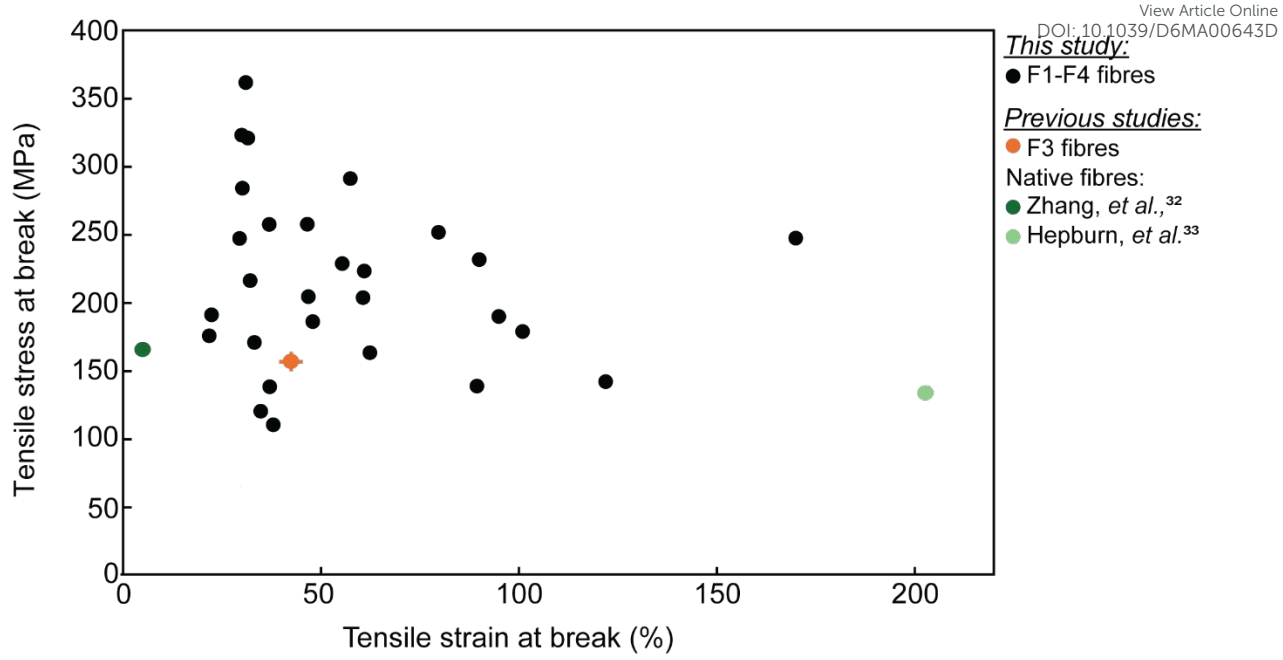

Figure 4. Tensile stress and tensile strain of recombinant silk fibres compared to previous data from continuously produced fibres from F3 and native fibres.

Implications for the development of biomaterials

Although heat-induced covalent cross-linking of protein materials has been known since the 1970s it has received relatively limited attention as a processing strategy for biomaterials.[35] Thermal treatment offers several advantages over chemical cross-linking approaches, most notably the avoidance of foreign reagents. By maintaining the material closer to its native chemical composition, thermal cross-linking is more likely to preserve biocompatibility and reduce the risk of adverse immune responses, which may simplify regulatory approval for clinical or commercial applications. [36-37] In addition, eliminating synthetic cross-linkers improves the environmental sustainability of the manufacturing process and avoids concerns associated with residual chemicals in the final material.[38]

A key consideration for the use of heat as a cross-linking strategy is its potential impact on protein structure. Previous work by Huson *et al.*[26] demonstrated that heat treatment (190 °C, 60 min) of F3-based silk materials resulted in limited secondary structural changes, with a gradual transition away from coiled coil structure towards β-sheet content. This transition was modest, reaching approximately 5% after ten minutes and 12% after one hour of treatment. In the present study, the very short thermal exposure required to induce covalent

View Article Online
DOI: 10.1039/D6MA00643D

cross-linking (approximately one minute) falls well within a regime that stabilises the material while minimising undesirable alterations to its final structural organisation and avoiding other chemical changes that may occur with long thermal treatments. These findings highlight the existence of a practical processing window in which thermal treatment can enhance material stability without compromising the designed protein architecture.

Conclusion

Previous studies have established recombinant aculeate silk proteins as promising platforms for both structural fibres[25] and a wide range of functional materials enabled by rational molecular design.[17-22,24] However, these earlier approaches relied exclusively on materials fabricated from individual silk protein components. Recent studies have shown that all four silk proteins found in native aculeate silk fold into stable coiled coil structures in solution.[12] In this study, we demonstrate that materials generated from all four silk proteins with iso-peptide thermal cross-links have markedly improved properties to those generated from a single protein and more closely resemble the performance of the natural system. Materials fabricated from the multi-protein heterotetrameric coiled coil assemblies exhibited up to 150% increases in strength and/or elasticity compared to materials generated from single protein components. Importantly, these materials could be rapidly cross-linked using short thermal treatments, producing robust, load-bearing networks while preserving the underlying coiled coil secondary structure present in the soluble protein state. Preservation of this structure ensures retention of the atomic-scale spatial organisation of the proteins, which underpins the reproducibility and reliability of material performance. Beyond this study, maintenance of the coiled coil architecture provides a stable structural framework for the rational incorporation of functional or environmentally responsive motifs to create new biofunctional materials without compromising material integrity.

These findings highlight the central role of cooperative protein assembly in governing structural stability and mechanical performance in aculeate silk-derived materials. By recapitulating the full protein composition of the native system, it is possible to overcome limitations previously encountered in recombinant silk materials and achieve native-like behaviour alongside enhanced mechanical performance and processability. Collectively, this work advances our understanding of how multi-component protein architectures can be

leveraged in materials design and provides a strong foundation for the rational engineering of complex, multifunctional protein-based biomaterials.

Author Contributions

Briggs - Writing – original draft, Writing – review & editing, Validation, Investigation, Methodology, Formal analysis

Michie - Validation, Investigation, Methodology

Liu - Investigation, Methodology, Formal analysis

Thomas - Methodology, Formal analysis

Cantor - Methodology, Formal analysis

Poole - Methodology, Formal analysis

Sutherland - Writing – original draft, Writing – review & editing, Conceptualisation, Visualisation, Investigation, Formal analysis, Supervision

Johnston - Writing – review & editing, Visualisation, Validation, Investigation, Formal analysis, Supervision

Conflicts of Interest

There are no conflicts to declare

Data Availability

Data available upon request from the corresponding author

Acknowledgements

This research used NCRIS-enabled Australian Proteome Analysis Facility (APAF) infrastructure

FTIR analysis was facilitated by access to the Research School of Chemistry, ANU.

View Article Online
DOI: 10.1039/D6MA00643D

References

1. S. M. Mithieux, S. G. Wise and A. S. Weiss, **Adv. Drug Deliv. Rev.**, 2013, **65**, 421–428.

2. S. M. Sweeney, J. P. Orgel, A. Fertala, J. D. McAuliffe, K. R. Turner, G. A. Di Lullo, S. Chen, O. Antipova, S. Perumal, L. Ala-Kokko, A. Forlino, W. A. Cabral, A. M. Barnes, J. C. Marini and J. D. San Antonio, **J. Biol. Chem.**, 2008, **283**, 21187–21197.

3. J. A. Werkmeister and J. A. M. Ramshaw, **Biomed. Mater.**, 2012, **7**, 012002.

4. T. D. Sutherland, M. G. Huson and T. D. Rapson, **J. Struct. Biol.**, 2018, **201**, 76–83.

5. T. D. Sutherland, J. Young, S. Weisman, C. Y. Hayashi and D. Merrit, **Annu. Rev. Entomol.**, 2010, **55**, 171–188.

6. T. D. Sutherland, H. E. Trueman, A. A. Walker, S. Weisman, P. M. Campbell, Z. Dong, M. G. Huson, A. L. Woodhead and J. S. Church, **J. Struct. Biol.**, 2014, **186**, 402–411.

7. M. Xu and R. V. Lewis, **Proc. Natl. Acad. Sci. U. S. A.,** 1990, **87**, 7120–7124.

8. Y. Cheng, L. D. Koh, D. Li, B. Ji, M. Y. Han and Y. W. Zhang, J**. R. Soc. Interface**, 2014, **11**, 20140305.

9. T. D. Sutherland, S. Weisman, T. E. Trueman, A. Sriskantha, J. W. H. Trueman and V. S. Haritos, **Mol. Biol. Evol.**, 2007, **24**, 2424–2432.

10. H. Sezutsu, H. Kajiwara, K. Kojima, K. Mita, T. Tamura, Y. Tamada and T. Kameda, **Biosci. Biotechnol. Biochem.,** 2007, **71**, 2725–2734.

11. K. M. Rudall, in **Comparative Biochemistry: A Comprehensive Treatise**, vol. 4, *Constituents of Life – Part B*, ed. M. Florkin and H. S. Mason, Academic Press, New York, 1962, pp. 397–433.

12. C. L. Johnston, J. Chacko, L. J. Briggs, M. Michie, J.-W. Liu, C. J. Morton, A. C. Warden and T. D. Sutherland, **Protein Sci.**, 2025, **34**, e70230.

13. P. M. Campbell, H. E. Trueman, Q. Zhang, K. Kojima, T. Kameda and T. D. Sutherland, **Insect Biochem. Mol. Biol.**, 2014, **48**, 40–50.

14. S. Weisman, V. S. Haritos, J. S. Church, M. G. Huson, S. T. Mudie, A. J. W. Rodgers, G. J. Dumsday and T. D. Sutherland, **Biomaterials**, 2010, **31**, 2695–2700.

15. P. J. Shilling, L. Pontes-Braz, L. Mitchell, L. Howell, P. Veneer, S. Jayashree, L. A. Castelli, T. Pham, L. Lu, B. Wand, B. Yeo, S. Nimma, L. Briggs, C. L. Johnston, M. Michie and T. D. Sutherland, **Protein Expr. Purif.**, 2025, **229**, 106683.

16. A. A. Walker, C. Holland and T. D. Sutherland, **Proc. R. Soc. B**, 2015, **282**, 20150259.

17. T. D. Rapson, T. D. Sutherland, J. S. Church, H. E. Trueman, H. Dacres and S. C. Trowell, **ACS Biomater. Sci. Eng.**, 2015, **1**, 1114–1120.

18. T. D. Rapson, J.-W. Liu, A. Sriskantha, M. Musameh, C. J. Dunn, J. S. Church, A. Woodhead, A. Warden, M. J. Riley, J. R. Harmer, C. J. Noble and T. D. Sutherland, **J. Inorg. Biochem.**, 2017a, **117**, 219–227.

19. T. D. Rapson, G. L. Hall and T. D. Sutherland, **J. Asthma**, 2019, **56**, 910–913.

20. M. M. Musameh, C. J. Dunn, M. H. Uddin, T. D. Sutherland and T. D. Rapson, **Biosens. Bioelectron.**, 2018, **103**, 26–31.

21. T. D. Rapson, R. Kusuoka, J. Butcher, M. Musameh, C. J. Dunn, J. S. Church, A. Warden, C. F. Blanford, N. Nakamura and T. D. Sutherland, **J. Mater. Chem. A**, 2017b, **5**, 10236–10243.

22. T. D. Rapson, A. M. Christley-Balcomb, C. J. Jackson and T. D. Sutherland, **J. Inorg. Biochem.**, 2020a, **204**, 110960.

23. C. C. Horgan, Y.-S. Han, H. Trueman, C. J. Jackson, T. D. Sutherland and T. D. Rapson, **RSC Adv.**, 2016, **6**, 39530–39533.

24. T. D. Rapson, H. Ju, P. Marshall, R. Devilla, C. J. Jackson, S. Giddey and T. D. Sutherland, **Sci. Rep.**, 2020b, **10**, 3774.

25. J. M. Poole, J. S. Church, A. L. Woodhead, M. G. Huson, A. Sriskantha, I. L. Kyratzis and T. D. Sutherland, **Macromol. Biosci.**, 2013, **13**, 1321–1326.

26. M. G. Huson, J. S. Church, J. M. Poole, S. Weisman, S. Sriskantha, A. C. Warden, P. M. Campbell, J. A. M. Ramshaw and T. D. Sutherland, **PLoS One**, 2012, **7**, e52308.

27. T. D. Sutherland, J. S. Church, X. Hu, M. G. Huson, D. L. Kaplan and S. Weisman, **PLoS One**, 2011, **6**, e16489.

28. S. A. Cohen and D. P. Michaud, **Anal. Biochem.**, 1993, **211**, 279–287.

29. T. D. Sutherland, S. Weisman, A. A. Walker and S. T. Mudie, **Biopolymers**, 2012, **97**, 446–454.

30. B. Audoly and J. W. Hutchinson, **J. Mech. Phys. Solids**, 2016, **97**, 68–91.

31. C. L. Johnston, L. J. Briggs, A. Kita, T. D. Sutherland, M. Michie, M. Velasque, Z. Kopecki and A. Antipov, **Adv. Healthcare Mater.**, 2026, submitted for publication

32. K. Zhang, F.-W. Si, H.-L. Duan and J. Wang, **Acta Biomater.**, 2010, **6**, 2165–2171.

33. H. R. Hepburn, H. D. Chandler and M. R. Davidoff, **Insect Biochem.**, 1979, **9**, 69–77.

34. S. Chen, M. Liu, H. Huang, L. Cheng and H. P. Zhao, **Mater. Des.**, 2019, **181**, 108077.

35. M. Otterburn, M. Healy and W. Sinclair, in **Protein Crosslinking**, ed. M. Friedman, *Advances in Experimental Medicine and Biology*, vol. 86, Springer, New York, 1977, pp. 239–262.

36. L. H. H. Olde Damink, P. J. Dijkstra, M. J. A. van Luyn, P. B. van Wachem, P. Nieuwenhuis and J. Feijen, **J. Mater. Sci: Mater. Med**, 1995, 6, 406-472.

37. H. W. Sung, D-M. Huang, W-H. Chang, R-N. Huang and J-C Hsu, J**. Biomed. Mater. Res**., 1999, 46, 520–530.

38. P. T. Anastas and J. C. Warner, Green Chemistry: Theory and Practice, Oxford University Press, New York, 2000.

1

View Article Online
DOI: 10.1039/D6MA00643D

CSIRO
CSIRO Black Mountain
Building 101, 2–40 Clunies Ross Street
Acton ACT 2601
Australia

View Article Online
DOI: 10.1039/D6MA00643D

4th May 2026

Dear Editor,

Data Availability Statement

- The data supporting this article have been included in text and as part of the Supplementary Information.

Yours sincerely,

Lyndall Briggs
(on behalf of all authors)

Commonwealth Scientific and Industrial Research Organisation,

Clunies Ross St, Black Mtn, Canberra ACT 2600
Lyndall.Briggs@CSIRO.au